JOURNAL OF THERMOPHYSICS AND HEAT TRANSFER
Vol. 8, No. 3, July–Sept. 1994

Finite Volume Method for Radiation Heat Transfer

John C. Chai*
University of Minnesota, Minneapolis, Minnesota 55455
HaeOk S. Lee†
NASA Lewis Research Center, Cleveland, Ohio 44135
and
Suhas V. Patankar‡
University of Minnesota, Minneapolis, Minnesota 55455

A finite volume method (FVM) is presented in this article. This procedure can be used to model transparent, absorbing, emitting, and anisotropically scattering media. A procedure to capture collimated beam is also presented. The FVM is applied to six test problems, and the results compared favorably against other published results. The test problems include two- and three-dimensional enclosures with participating media, collimated incidence, and heat generation. The efficiency of the FVM procedure is also investigated using a three-dimensional test problem.

Nomenclature

a	= coefficient in the discretization equation, Eqs. (13) and (14)
b	= source term in the discretization equation, Eqs. (13) and (14)
D^l_{cx}, D^l_{cy}	= defined quantities, Eq. (10a)
D_x, D_y	= x and y direction enclosure lengths
d^l	= distance traveled between an upstream location and a control volume face
G	= incident radiation, $\int_{4\pi} I \, d\Omega$
G^*	= dimensionless G, $G/(4\sigma T_h^4)$
I	= actual intensity
M	= total number of ordinates
$\hat{n}$	= outward normal of the control volume faces
$\hat{n}_x$	= unit vector normal to the x = const line
$\hat{n}_y$	= unit vector normal to the y = const line
q	= heat flux, $\int_{2\pi} I(\hat{s}\cdot\hat{n}_i) \, d\Omega$
q_c	= heat flux due to collimated beam
q_{gen}	= heat source, Eq. (18)
q^*	= dimensionless heat flux, $q/\sigma T_g^4$
q^{**}	= dimensionless heat flux, q/q_c
q^{***}	= dimensionless heat flux, $q/\sigma(T_h^4 - T_c^4)$
S	= source function, Eq. (2b)
S_C, S_P	= coefficients in Eq. (23)
S^l_m	= modified source function, Eq. (7b)
s	= distance traveled by a beam
$\hat{s}$	= unit direction vector
T	= temperature
w	= angular weights
x, y, z	= coordinate directions
β	= extinction coefficient, $\kappa + \sigma$
β^l_m	= modified extinction coefficient, Eq. (7a)
ΔA	= area of control volume faces
Δv	= volume of the control volume
Δx, Δy	= x and y direction control volume widths
$\Delta\Omega$	= control angle, Eq. (10c)
ε	= emissivity
θ	= polar angle, Figs. 1 and 2
κ	= absorption coefficient
μ, ξ	= x and y direction cosines
σ	= scattering coefficient or Stefan-Boltzmann constant
Φ	= scattering phase function
$\Phi^{l'l}$	= average scattering phase function, Eq. (22)
ϕ	= azimuthal angle, Figs. 1 and 2

Subscripts

b	= blackbody
c	= cold or collimated
E, W, N, S	= east, west, north, and south neighbors of P
e, w, n, s	= east, west, north, and south control volume faces
g	= gas
h	= hot
P	= control volume
x, y, z	= coordinate directions

Superscript

l, l'	= angular directions

Introduction

OVER the last two decades, the control volume approach[1] has emerged as a popular fluid flow solution procedure. This approach has been applied to model a variety of fluid flow and heat transfer related processes, which include electronic cooling, combustion chambers, and greenhouses. Radiation can be an important heat transfer mode in some of these applications. Therefore, it is desirable to employ a radiation heat transfer procedure which shares the same computational grid and philosophy with the control volume method. The same computational grid is used mainly for convenience because this eliminates the need to interpolate temperature, absorption coefficient, scattering coefficient, and average intensity during the iteration process.

The discrete ordinates method[2-5] is a radiation calculation procedure which shares a computational grid with the control volume approach. This method solves the equation of transfer by replacing the integration for the scattering source term by

Presented as Paper 93-2731 at the AIAA 28th Thermophysics Conference, Orlando, FL, July 6–9, 1993; received July 23, 1993; revision received Dec. 6, 1993; accepted for publication Jan. 24, 1994.

*Ph.D. Candidate, Department of Mechanical Engineering. Student Member AIAA.

†Aerospace Engineer, Propulsion Systems Division. Senior Member AIAA.

‡Professor, Department of Mechanical Engineering.

a quadrature sum and discretizing it into a set of coupled algebraic equations.

There are many ways of choosing a quadrature set consisting of ordinates and weights.[3-5] A quadrature set is obtained by applying appropriate constraints, e.g., symmetry and moments matching. In modeling radiative transfer, a carefully chosen quadrature set should satisfy the full-range zeroth moment, half- and full-range first moments, as well as some higher-order moments.[5]

Recently, Raithby and co-workers[6-8] presented new angular and spatial discretization practices. In this approach, radiant energy is conserved within a control angle, control volume, and globally for *any* number of control angles and control volumes arranged in *any* manner.

The objective of this article is to present a finite volume radiation heat transfer calculation procedure compatible with the control volume approaches of Karki and Patankar,[9-11] Demirdzic et al.,[12] Peric,[13] Shyy et al.,[14] and Rhie and Chow.[15] The step and modified-exponential[16] schemes are used. In this article, formulation for a two-dimensional Cartesian coordinate system is presented for simplicity and clarity. Formulation for curvilinear coordinates is presented in a following paper.[17]

The remainder of this article is divided into three sections. The governing equation and the finite volume method (FVM) is presented in detail. This is followed by the presentation and discussion of six test problems. Both two- and three-dimensional enclosures are considered. The three-dimensional enclosure problem is used to investigate the computational efficiency of FVM. Finally, some concluding remarks are presented.

Formulation of the Discretization Equation

The equation of transfer can be written as[18]

$$\frac{dI(r, \hat{s})}{ds} = -\beta(r)I(r, \hat{s}) + S(r, \hat{s}) \tag{1}$$

where the extinction coefficient and the source function are

$$\beta(r) = \kappa(r) + \sigma(r) \tag{2a}$$

$$S(r, \hat{s}) = \kappa(r)I_b(r, \hat{s}) + \frac{\sigma(r)}{4\pi}\int_{4\pi} I(r, \hat{s}')\Phi(\hat{s}', \hat{s})\, d\Omega' \tag{2b}$$

In Eqs. (1) and (2), $\boldsymbol{r}$ is the position vector and $\hat{s}$ is the unit vector describing the radiation direction.

Equation (1) indicates that intensity depends on spatial position and angular direction. To discretize Eq. (1), a finite volume practice is used. The control angles used in this study are the *solid angles* proposed and used by Raithby and co-workers.[6-8] In a ray effect study, Brigg et al.[19] presented a piecewise constant discrete ordinates-like angular finite element algorithm. Following the control volume spatial discretization practice, the angular space is subdivided into $N_\theta \times N_\phi = M$ control angles. Analogous to the placement of control volumes (see Fig. 1a), a user has the freedom to place the control angles in any desired manner. Figure 1b depicts a sample angular discretization using a unit hemisphere.

Integrating Eq. (1) over a typical two-dimensional Δv and $\Delta\Omega^l$ gives

$$\int_{\Delta\Omega^l}\int_{\Delta v} \frac{dI^l}{ds}\, dv\, d\Omega^l = \int_{\Delta\Omega^l}\int_{\Delta v} (-\beta I^l + S^l)\, dv\, d\Omega^l \tag{3}$$

where $I^l \equiv I(r, \hat{s}^l)$. Applying the divergence theorem, Eq. (3) becomes

$$\int_{\Delta\Omega^l}\int_{\Delta A} I^l(\hat{s}^l\cdot\hat{n})\, dA\, d\Omega^l = \int_{\Delta\Omega^l}\int_{\Delta v} (-\beta I^l + S^l)\, dv\, d\Omega^l \tag{4}$$

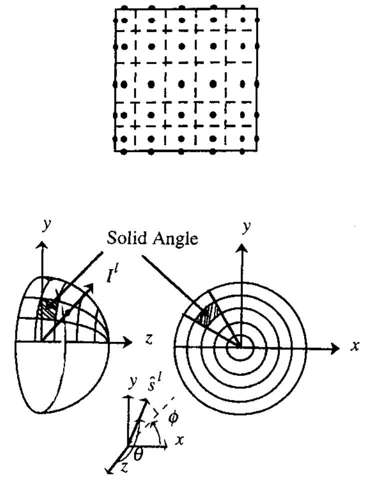

Fig. 1 Samples spatial and angular discretizations: a) control volumes and b) control or solid angle.

The left side of Eq. (4) represents the inflow and outflow of radiant energy across the four control volume faces. The right side denotes the attenuation and augmentation of energy within a control volume. Following the practice of the control volume approach, the intensity is assumed constant within a control volume *and* a control angle. Under these assumptions, Eq. (4) can be simplified to

$$\sum_{i=1}^{4} I_i^l \Delta A_i \int_{\Delta\Omega^l} (\hat{s}^l\cdot\hat{n}_i)\, d\Omega^l = (-\beta I^l + S^l)\Delta v \Delta\Omega^l \tag{5}$$

where

$$S^l = \kappa I_b + \frac{\sigma}{4\pi}\sum_{l'=1}^{M} I^{l'}\bar{\Phi}^{l'l}\Delta\Omega^{l'} \tag{6}$$

In Eq. (6), $\bar{\Phi}^{l'l}$ is the average scattering phase function from control l' to control angle l, later defined in the Sample Applications: Anisotropic Scattering Medium section.

In Eq. (5), the radiation direction varies within a control angle, whereas the magnitude of the intensity is assumed constant. If the radiation direction is fixed at a given direction within a control angle and the magnitude of the intensity is also constant, the discretization equation for the discrete ordinates method[16] is obtained.

Following the treatment presented by Chai et al.,[16] a modified extinction coefficient and a modified source function can be written for a discrete direction l as

$$\beta_m^l = \beta - \frac{\sigma}{4\pi}\bar{\Phi}^{ll}\Delta\Omega^l \tag{7a}$$

$$S_m^l = \kappa I_b + \frac{\sigma}{4\pi}\sum_{l'=1, l'\neq l}^{M} I^{l'}\bar{\Phi}^{l'l}\Delta\Omega^{l'} \tag{7b}$$

With this modification, Eq. (5) becomes

$$\sum_{i=1}^{4} I_i^l \Delta A_i \int_{\Delta\Omega^l} (\hat{s}^l\cdot\hat{n}_i)\, d\Omega^l = (-\beta_m^l I^l + S_m^l)\Delta v \Delta\Omega^l \tag{8}$$

For the typical control volume and radiation direction shown in Fig. 2a, Eq. (8) can be further simplified to

$$(I_e^l - I_w^l)\Delta A_x D_{cx}^l + (I_n^l - I_s^l)\Delta A_y D_{cy}^l = [-(\beta_m^l)_P I_P^l + (S_m^l)_P]\Delta v \Delta\Omega^l \tag{9}$$

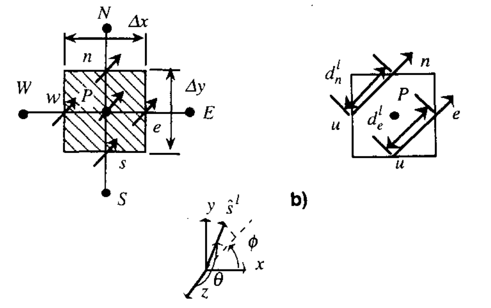

Fig. 2 Some useful definitions: a) typical control volume and radiation direction and b) distances traveled by a radiation beam.

where

$$D^l_{cx} = \int_{\Delta\Omega^l} (\hat{s}^l \cdot \hat{n}_x)\, d\Omega^l, \qquad D^l_{cy} = \int_{\Delta\Omega^l} (\hat{s}^l \cdot \hat{n}_y)\, d\Omega^l \tag{10a}$$

$$\Delta A_x = \Delta y, \qquad \Delta A_y = \Delta x \tag{10b}$$

$$\Delta v = \Delta x \Delta y, \qquad \Delta\Omega^l = \int_{\phi^{l-}}^{\phi^{l+}} \int_{\theta^{l-}}^{\theta^{l+}} \sin\theta \, d\theta \, d\phi \tag{10c}$$

To relate the boundary intensities to the nodal intensity, spatial differencing schemes are needed. One available scheme is the step scheme which sets the downstream boundary intensities equal to the upstream nodal intensities; $I^l_n = I^l_e = I^l_P$, $I^l_w = I^l_W$, and $I^l_s = I^l_S$. For the situation depicted in Fig. 2a, the step scheme discretization equation can be written as

$$I^l_P = \frac{\Delta y D^l_{cx} I^l_W + \Delta x D^l_{cy} I^l_S + (S^l_m)_P \Delta v \Delta\Omega^l}{\Delta y D^l_{cx} + \Delta x D^l_{cy} + (\beta^l_m)_P \Delta v \Delta\Omega^l} \tag{11}$$

Equation (11) is similar to the discretization equation for the S_n discrete ordinates method.[16] As a matter of fact, the discretization equation for the S_n discrete ordinates method is obtained by replacing D^l_{cx} with μ, D^l_{cy} with ξ, deleting $\Delta\Omega^l$ from the numerator and denominator of Eq. (11), and replacing $\Delta\Omega^l$ with w^l in Eqs. (7a) and (7b).

A study of different spatial differencing schemes by Chai et al.[20] indicates that control volume boundary intensities should be calculated by tracing a beam to an appropriate upstream location where the intensity is known or can be approximated. Raithby and co-workers[6–8] used a higher-order profile, and the upstream intensities were obtained by interpolations of known upstream intensities. The modified-exponential scheme[16] is used in the present study. In this study, the upstream intensities I^l_u for both the north and east boundary intensities, are approximated as I^l_P. The boundary intensities are then evaluated using the modified-exponential scheme as

$$I^l_e = I^l_P e^{-(\beta^l_m)_P d^l_e} + \left(\frac{S^l_m}{\beta^l_m}\right)_P \left(1 - e^{-(\beta^l_m)_P d^l_e}\right) \tag{12}$$

where $(S^l_m)_P$ and $(\beta^l_m)_P$ are given in Eq. (7). The distance d^l_e is shown in Fig. 2b. The I^l_u for the west, north, and south boundaries are I^l_W, I^l_P, and I^l_S, respectively. Similar expressions can be written for these boundary intensities.

Using these profiles, the final discretization equation for the nodal intensity for the $D^l_{cx} > 0$ and $D^l_{cy} > 0$ conditions can be written as

$$a^l_P I^l_P = a^l_W I^l_W + a^l_S I^l_S + b^l \tag{13}$$

where

$$a^l_W = \Delta A_x D^l_{cx} e^{-(\beta^l_m)_W d^l_w}, \qquad a^l_S = \Delta A_y D^l_{cy} e^{-(\beta^l_m)_S d^l_s} \tag{14a}$$

$$a^l_P = \Delta A_y D^l_{cy} e^{-(\beta^l_m)_P d^l_n} + \Delta A_x D^l_{cx} e^{-(\beta^l_m)_P d^l_e} + (\beta^l_m)_P \Delta v \Delta\Omega^l \tag{14b}$$

$$\begin{aligned} b^l = {} & (S^l_m)_P \Delta v \Delta\Omega^l + \left(\frac{S^l_m}{\beta^l_m}\right)_W \Delta A_x D^l_{cx}\left[1 - e^{-(\beta^l_m)_W d^l_w}\right] \\ & + \left(\frac{S^l_m}{\beta^l_m}\right)_P \Delta A_x D^l_{cx}\left[1 - e^{-(\beta^l_m)_P d^l_s}\right] - \left(\frac{S^l_m}{\beta^l_m}\right)_P \{\Delta A_x D^l_{cx} \\ & \times \left[1 - e^{-(\beta^l_m)_P d^l_n}\right] + \Delta A_x D^l_{cx}\left[1 - e^{-(\beta^l_m)_P d^l_e}\right]\} \end{aligned} \tag{14c}$$

For the first internal control volumes, the boundary points are the neighbor nodal points (see Fig. 2a).

The source term, b^l in Eq. (14c), can become negative and lead to physically incorrect negative nodal intensity when the magnitude of the negative source term is large. The always-positive variable treatment of Patankar[1] is used to eliminate this possibility. Using this procedure, b^l and coefficient a^l_P from Eqs. (14b) and (14c) are rearranged as

$$\begin{aligned} a^l_P = {} & \Delta A_y D^l_{cy} e^{-(\beta^l_m)_P d^l_n} + \Delta A_x D^l_{cx} e^{-(\beta^l_m)_P d^l_e} + (\beta^l_m)_P \Delta v \Delta\Omega^l \\ & + \left(\frac{1}{I^{l0}_P}\right)\left(\frac{S^l_m}{\beta^l_m}\right)_P \{\Delta A_x D^l_{cx}\left[1 - e^{-(\beta^l_m)_P d^l_n}\right] \\ & + \Delta A_x D^l_{cx}\left[1 - e^{-(\beta^l_m)_P d^l_e}\right]\} \end{aligned} \tag{15a}$$

$$\begin{aligned} b^l = {} & (S^l_m)_P \Delta v \Delta\Omega^l + \left(\frac{S^l_m}{\beta^l_m}\right)_W \Delta A_x D^l_{cx}\left[1 - e^{-(\beta^l_m)_W d^l_w}\right] \\ & + \left(\frac{S^l_m}{\beta^l_m}\right)_P \Delta A_x D^l_{cx}\left[1 - e^{-(\beta^l_m)_P d^l_s}\right] \end{aligned} \tag{15b}$$

where I^{l0}_P is I^l_P from the previous iteration. Equations (13) and (14a), together with Eqs. (15a) and (15b), guarantee positive nodal intensity I^l_P. Similar expressions can be written for one- and three-dimensional Cartesian coordinate systems without any new concept and is left to the exploration of interested readers. The step scheme discretization equation [Eq. (11)] can be obtained from Eqs. (13–15) by setting all e^{-x} (x is the argument of the exponent) to unity.

In the solution of Eqs. (13–15), with appropriate boundary conditions, zero intensity or a suitable intensity field is used as an initial guess. The solution process is initiated with the $D^l_{cx} > 0$ and $D^l_{cy} > 0$ conditions by a marching process. This process is repeated for all other directions, and a solution is deemed converged when it satisfied the following constraint:

$$|I^l_P - I^{l0}_P| / I^l_P \leq 10^{-6} \tag{16}$$

Again, I^{l0}_P is the I^l_P from the previous iteration.

When the modified-exponential scheme is used, the solution process is initiated using the step scheme, and the modified-exponential scheme is activated after a reasonable intensity field is obtained using the step scheme. In this study, the modified-exponential scheme is activated when the intensity field satisfies

$$|I^l_P - I^{l0}_P| / I^l_P \leq 10^{-3} \tag{17}$$

Sample Applications

In this section, the FVM is applied to six test problems. Current results are compared with those in published literature.

Isothermal Absorbing-Emitting Medium

This problem consists of an absorbing-emitting medium maintained at a constant temperature T_g. The black, square

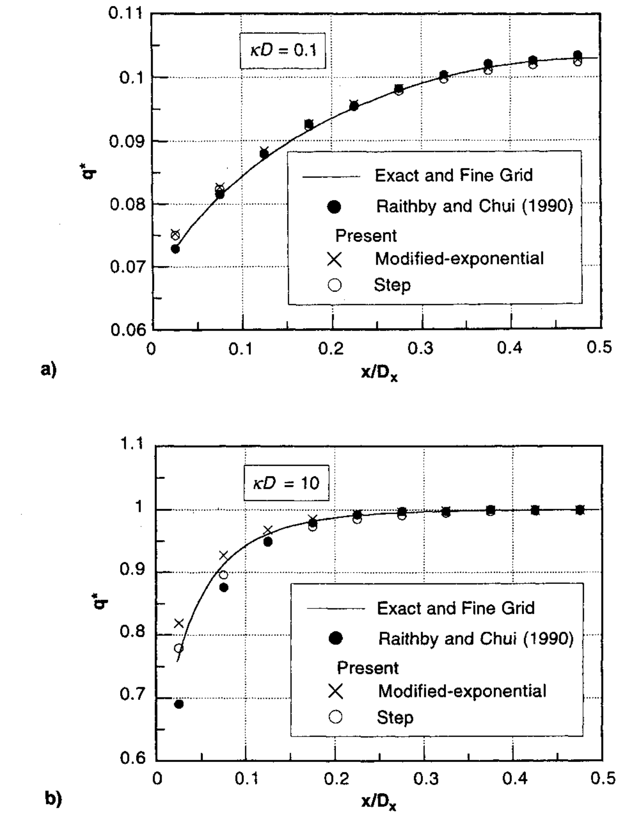

Fig. 3 Dimensionless heat flux along the bottom wall: a) $\kappa D = 0.1$ and b) $\kappa D = 10.0$.

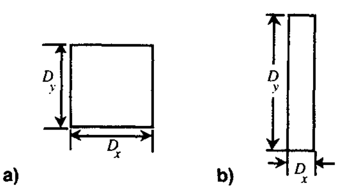

Fig. 4 Schematics of two test problems: a) $D_y/D_x = 1$ and b) $D_y/D_x = 10.0$.

enclosure is like that shown in Fig. 1a, and has cold walls kept at 0 K. This problem was studied by many researchers, Raithby and Chui,[6] Fiveland,[21] and Truelove,[22] just to name a few. Comparisons with the results of Raithby and Chui[6] for $\kappa D_x = \kappa D_y = 0.1$ and 10 are presented in Fig. 3.

The calculation domain is discretized into 20×20 uniform control volumes in the x and y directions, respectively. The step and modified-exponential schemes are used. For $\kappa D_x = \kappa D_y = 10$, two angular discretizations are used; 1×4 and 2×8 control angles with *uniform* $\Delta\theta$ and $\Delta\phi$ in the θ and ϕ directions, respectively. Finer angular discretizations are used for the optically thinner problem (1×12 and 2×24 control angles with uniform $\Delta\theta$ and $\Delta\phi$ in the θ and ϕ directions, respectively). These are the same control angles used by Raithby and Chui.[6]

Figure 3 shows the dimensionless heat fluxes on the bottom wall obtained using the finer angular grids. The results of the step and modified-exponential schemes are in good agreement with the exact and Raithby and Chui's solutions. The results obtained using these schemes are very reasonable. The coarse angular grid, although not shown, also produced accurate solutions.

Purely Scattering Problems

Figure 4 shows schematics of two geometries with aspect ratios, $D_y/D_x = 1$ and 10. Bottom walls of the enclosures are hot at T_h, with the remaining walls maintained at $T_c = 0$ K. The medium scatters energy isotropically, and the scattering albedo ($\omega = \sigma/\beta$) is taken as unity.

The dimensionless heat flux on the hot wall, and the dimensionless centerline incident radiation are plotted in Fig. 5. Figure 5a shows the dimensionless heat flux for the square enclosure. When coarse grid is used, the step scheme overpredicts the heat flux, but it approaches the exact solution of Crosbie and Schrenker[23] with grid refinement. The modified-exponential scheme produces more accurate solution with a coarse grid, and the solution approaches the exact solution quicker. It should be pointed out that the finite volume method of Raithby and Chui[6] reproduce the exact solution more accurately with the computational grids listed in Fig. 5.

Figure 5b shows the dimensionless incident radiation at $x/D_x = 0.5$ for $D_y/D_x = 10$. Both the step and the modified-exponential schemes produce accurate G^* distributions.

Three-Dimensional Heat Generation Problems

The three-dimensional idealized furnace of Menguc and Viskanta[24] is chosen as the next test problem. Figure 6a shows the physical problem considered. The enclosure is filled with an absorbing-emitting medium with $\kappa = 0.5\ \mathrm{m}^{-1}$. The temperature distribution is determined from the following energy equation with a heat source of $q_{gen} = 5\ \mathrm{kW/m}^3$

$$\nabla \cdot q = q_{gen} = \kappa(4\pi I_b - G) \tag{18}$$

The boundary conditions are

$$z = 0, \qquad T = 1200\ \mathrm{K}, \qquad \varepsilon = 0.85 \tag{19a}$$

$$z = 4\ \mathrm{m}, \qquad T = 400\ \mathrm{K}, \qquad \varepsilon = 0.70 \tag{19b}$$

$$\text{others}, \qquad T = 900\ \mathrm{K}, \qquad \varepsilon = 0.70 \tag{19c}$$

Figure 6b shows the temperature distributions at $y = 1$ m. These solutions were obtained using $25 \times 25 \times 25$ uniform control volumes, and 4×20 control angles. The results are in good agreement with the zone method and the S_4 discrete ordinates solution of Fiveland[25] (except at $z = 0.4$ m). So-

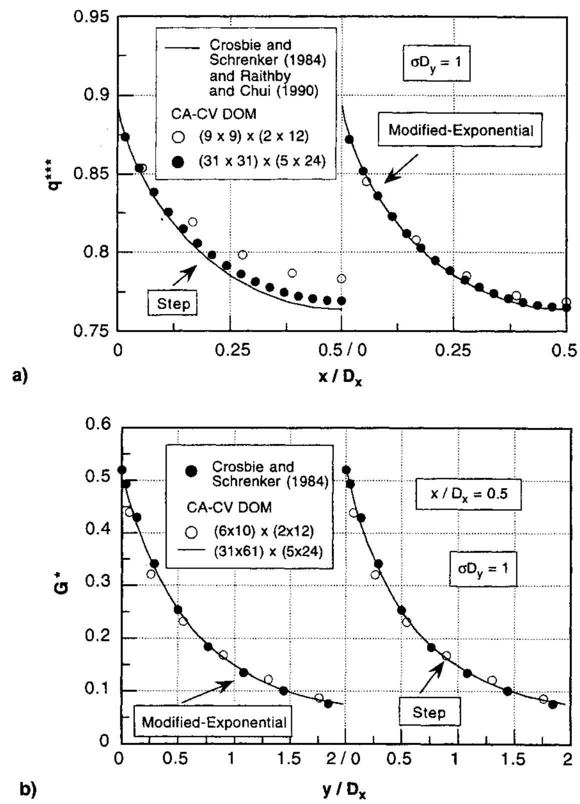

Fig. 5 Isotropically scattering media: a) dimensionless heat flux for $D_y/D_x = 1$ and b) dimensionless centerline average intensity for $D_y/D_x = 10$.

Table 1 Comparisons of CPU times (s) and number of iterations between the FVM and the S_n DOM

Case	κ	σ, isotropic	$N_x \times N_y \times N_z = 7 \times 7 \times 11$		$N_x \times N_y \times N_z = 20 \times 20 \times 20$	
			FVM $(2 \times 12)^b/S_4$	FVM $(4 \times 20)^b/S_8$	FVM $(2 \times 12)^b/S_4$	FVM $(4 \times 20)^b/S_8$
(a)	0.5	0.0	0.56 (18)/0.50 (18)	1.18 (18)/1.03 (18)	4.45 (18)/4.87 (18)	11.76 (18)/12.46 (18)
(b)	1.0	0.0	0.83 (29)/0.76 (29)	1.82 (29)/1.62 (29)	7.75 (30)/8.06 (30)	20.3 (30)/20.7 (30)
(c)	0.5	0.5	1.80 (29)/1.25 (29)	7.99 (29)/4.16 (29)	22.70 (30)/15.68 (30)	115.18 (30)/57.63 (30)
(d)	0.0	1.0	1.77 (29)/1.22 (29)	7.93 (29)/4.13 (29)	21.40 (30)/15.19 (30)	114.00 (30)/57.11 (30)
(e)[a]	0.0	1.0	1.26 (20)/0.85 (20)	5.50 (20)/2.86 (20)	14.8 (20)/10.51 (20)	76.00 (20)/39.30 (20)

[a]The right side of Eq. (16) was set to 10^{-4}. [b]The first two numbers represent $N_\theta \times N_\phi$.

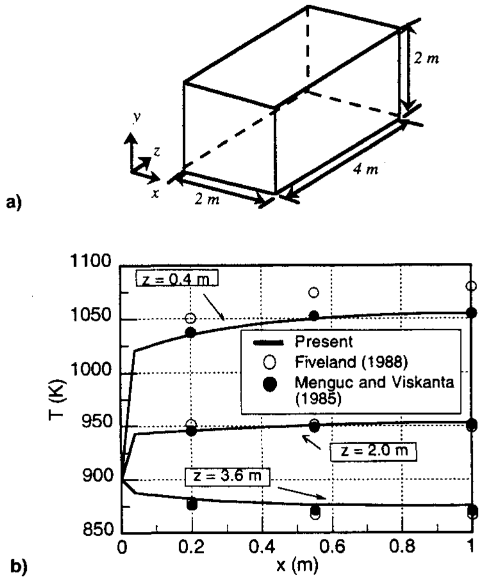

Fig. 6 An idealized furnace: a) schematic and b) temperature distributions at y = 1 m.

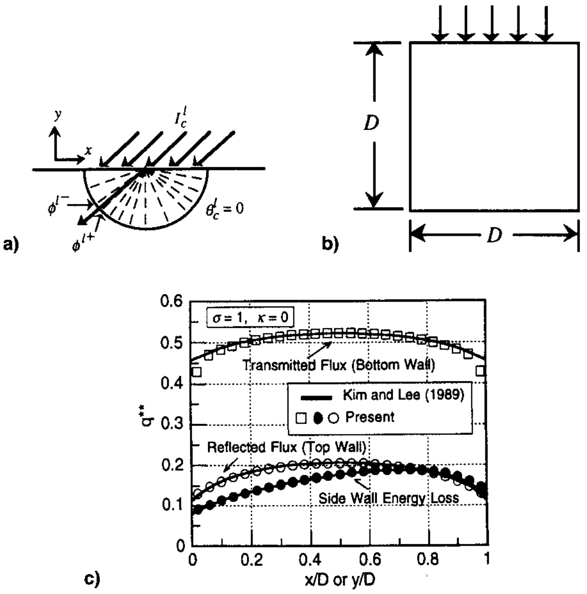

Fig. 7 Collimated incidence problem: a) possible control angle arrangement, b) schematic, and c) dimensionless heat fluxes.

lutions with coarser angular and spatial grids, although not shown in the figure, also produce similar accuracy. The FVM was also applied to the κ = 0.25 and 1.0 m^{-1} test cases, and accurate solutions were also obtained.[26]

This furnace problem is modified to investigate the efficiency of the FVM. Table 1 lists the Cray-C90's CPU times and the number of iterations (in parentheses) needed to obtain converged solutions for five cases. The CPU times for the S_n discrete ordinates method (DOM) are also listed for comparisons. For this efficiency study, the enclosure walls are assumed black to minimize the number of governing parameters. Solutions for cases (a–d) are assumed converged when Eq. (16) is satisfied. In case (e), the solution is assumed to be converged when the left side of Eq. (16) is less than 10^{-4}.

In terms of the number of iterations, the FVM is as efficient as the S_n DOM. In terms of CPU times, the FVM is as efficient as the S_n DOM for nonscattering media computations. In isotropically scattering media, the FVM requires anywhere between one and one-half to two times the CPU times of the S_n DOM for these test cases.

Collimated Incidence Problem

Since a user has freedom to arrange the control angles in any manner advantageous to the problem at hand, collimated incidence can be easily captured by matching the direction of the collimated beam. Therefore, the *actual* intensity is solved directly with the FVM. This feature is not available for the S_n discrete ordinates method, unless the direction of the collimated beam happens to coincide with an ordinate direction. Figure 7a shows a possible arrangement of control angles to capture a collimated beam, $\theta_c^l = 0$ for simplicity. Notice that the size of the control angle can be changed by adjusting ϕ^{l-} and ϕ^{l+}.

Figure 7b shows a schematic of a problem studied by Kim and Lee,[27] chosen to show the ability of the present procedure to model problems with collimated incidence. The top wall of the black enclosure is subjected to a normal collimated beam. The other walls are maintained at 0 K, and the medium scatters energy isotropically with a scattering albedo of unity. The domain is divided into 25 × 25 uniform control volumes and 3 × 24 control angles in the θ and ϕ directions. The step scheme is used in the present problem. The control angles are adjusted to capture the collimated incidence, and the actual intensity is solved. In this problem, $\phi^{l+} - \phi^{l-}$ shown in Fig. 7a, which corresponds to the particular ϕ^l in the direction of the collimated beam, was set to 2 deg. The remaining control angles can be arranged in any desired manner. Similar treatment is also used in the θ direction. Figure 7c shows good agreement between the present computation and the S_{14} discrete ordinates solution of Kim and Lee.[27]

Anisotropically Scattering Medium

When scattering is present in a medium, it is important to integrate the scattering phase function correctly. A scattering phase function obeys the following relation

$$\int_{4\pi} \Phi(\hat{s}', \hat{s})\, d\Omega = 4\pi \tag{20}$$

In the finite volume approach, this quantity is approximated as

$$\int_{4\pi} \Phi(\hat{s}', \hat{s})\, d\Omega' = \sum_{l'=1}^{L} \bar{\Phi}^{l'l} \Delta\Omega^{l'} \tag{21}$$

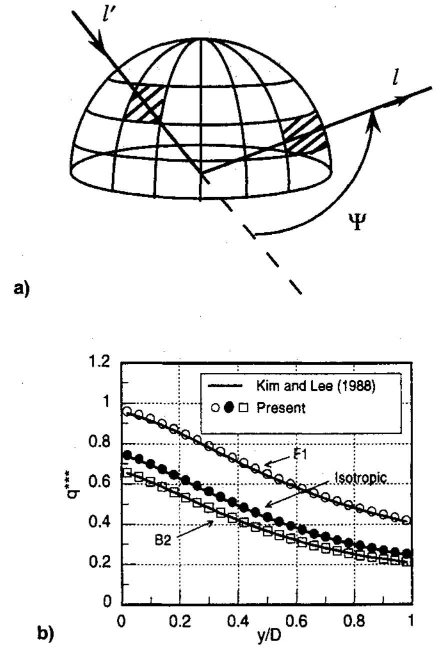

Fig. 8 Anisotropically scattering problems: a) scattering from control angle $\Delta\Omega^{l'}$ to $\Delta\Omega^{l}$ and b) dimensionless centerline heat flux.

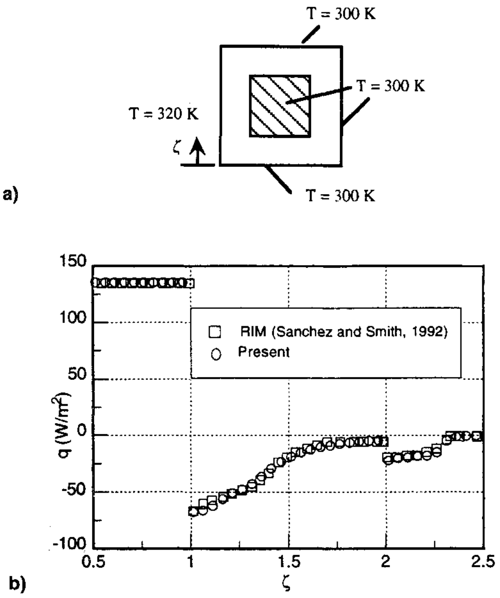

Fig. 9 An enclosure with a central block: a) schematic and b) local heat flux along the enclosure walls.

where $\bar{\Phi}^{l'l}$ represents the average energy scattered from control-angle l' to control-angle l (see Fig. 8a) and can be evaluated accurately from[7,8]

$$\bar{\Phi}^{l'l} = \frac{\int_{d\Omega}\int_{d\Omega'} \Phi(\hat{s}', \hat{s})\, d\Omega\, d\Omega'}{\Delta\Omega^{l}\Delta\Omega^{l'}} \tag{22}$$

A two-dimensional square enclosure problem for a purely scattering medium studied by Kim and Lee[28] is repeated. The black enclosure, with an optical depth of 1, has three cold walls and a hot bottom wall. A forward (F1), backward (B2), and isotropic phase functions are studied using 25 × 25 control volumes and 6 × 24 control angles. Figure 8b shows the centerline y-direction heat flux. The present solutions compare very well with the solutions of Kim and Lee.[28]

Irregular Geometry Problem

Chai et al.[29] presented treatments of irregular geometries using the S_n discrete ordinates methods. This treatment can be used to treat protrusions, obstructions and "cut-out" regions. Figure 9a shows a sample irregular geometry which can be modeled using the procedures described by Chai et al.[29] The obstruction is opaque to radiation and can reflect energy. The medium can absorb, emit, and scatter radiative energy. Since detailed analyses are available,[29] this section presents a summary of the procedure.

For ease of presentation, an additional source term is defined as

$$\bar{S} = S_C + S_P I_P^l \tag{23}$$

The coefficients S_C and S_P are given appropriate values to account for irregular geometries. To be consistent with the practice used in CFD, the coefficient S_P must be negative. The final discretization equation, using the step scheme, can be written as

$$I_P^l = \frac{\Delta y D_{cx}^l I_W^l + \Delta x D_{cy}^l I_S^l + [(S_m^l)_P + S_C]\Delta v \Delta\Omega^l}{\Delta y D_{cx}^l + \Delta x D_{cy}^l + [(\beta_m^l)_P - S_P]\Delta v \Delta\Omega^l} \tag{24}$$

From Eq. (24), it can be seen that the arrays for $(S_m^l)_P$ and $(\beta_m^l)_P$ can be used for S_C and S_P, respectively. Similar equation for the modified-exponential scheme can be written.

Figure 9a shows a problem studied by Sanchez and Smith,[30] with all walls assumed black. The known temperatures are shown in Fig. 9a, and the medium does not participate in the radiative heat transfer process. Figure 9b depicts the heat flux along the walls of the enclosure. The computation was performed using 40 × 40 uniform control volumes and 4 × 20 control angles in the θ and ϕ directions. The solution agrees well with the radiosity-irradiation model (RIM) solution presented by Sanchez and Smith.[30]

Concluding Remarks

A FVM is presented in this article. The FVM has been applied to transparent, absorbing, emitting, and anisotropically scattering media in two- and three-dimensional enclosures to illustrate its capabilities. The main advantage of the FVM procedure is that a user has complete flexibility in laying out the spatial and angular grids that best capture the physics of a given problem. The collimated beam example is used to illustrate this advantage. One irregular geometry test problem is also presented. All results demonstrated that the present procedure is accurate and efficient when compared with the S_n discrete ordinates method. Ray effect and false scattering encountered in the S_n discrete ordinates method[31] are also encountered with the finite volume method.

Acknowledgments

This work is supported in part by NASA Lewis Research Center under Cooperative Agreement Grant NCC3-238. A grant from the Minnesota Supercomputer Institute is also gratefully acknowledged.

References

[1]Patankar, S. V., *Numerical Heat Transfer and Fluid Flow*, McGraw-Hill, New York, 1980.

[2]Chandrasekhar, S., *Radiative Transfer*, Dover, New York, 1960.

[3]Carlson, B. G., and Lathrop, K. D., "Transport Theory—the Method of Discrete-Ordinates," *Computing Methods in Reactor Physics*, edited by H. Greenspan, C. N. Kelber, and D. Okrent, Gordon & Breach, New York, 1968.

[4]Lewis, E. E., and Miller, W. F., Jr., *Computational Methods of Neutron Transport*, Wiley, New York, 1984.

[5]Fiveland, W. A., "The Selection of Discrete Ordinate Quadrature Sets for Anisotropic Scattering," *Fundamentals of Radiation Heat Transfer*, 28th National Heat Transfer Conf., American Society of

Mechanical Engineers HTD-Vol. 160, 1992, pp. 89–96.

[6]Raithby, G. D., and Chui, E. H., "A Finite-Volume Method for Predicting a Radiant Heat Transfer in Enclosures with Participating Media," *Journal of Heat Transfer*, Vol. 112, No. 2, 1990, pp. 415–423.

[7]Chui, E. H., Raithby, G. D., and Hughes, P. M. J., "Prediction of Radiative Transfer in Cylindrical Enclosures with the Finite Volume Method," *Journal of Thermophysics and Heat Transfer*, Vol. 6, No. 4, 1992, pp. 605–611.

[8]Chui, E. H., and Raithby, G. D., "Computation of Radiant Heat Transfer on a Nonorthogonal Mesh Using the Finite-Volume Method," *Numerical Heat Transfer*, Vol. 23, Pt. B, 1993, pp. 269–288.

[9]Karki, K. C., and Patankar, S. V., "Calculation Procedure for Viscous Incompressible Flows in Complex Geometries," *Numerical Heat Transfer*, Vol. 14, 1988, pp. 295–307.

[10]Karki, K. C., and Patankar, S. V., "Solution of Some Two-Dimensional Incompressible Flow Problems Using a Curvilinear Coordinate System Based Calculation Procedure," *Numerical Heat Transfer*, Vol. 14, 1988, pp. 309–321.

[11]Karki, K. C., and Patankar, S. V., "Pressure-Based Calculation Procedure for Viscous Flows at All Speeds in Arbitrary Configurations," *AIAA Journal*, Vol. 27, No. 9, 1989, pp. 1167–1174.

[12]Demirdzic, I., Gosman, A. D., and Issa, R. I., "A Finite-Volume Method for the Prediction of Turbulent Flow in Arbitrary Geometries," *Lecture Notes in Physics*, Vol. 141, 1980, pp. 141–150.

[13]Peric, M., "A Finite Volume Method for the Prediction of Three Dimensional Fluid Flow in Complex Duct," Ph.D. Dissertation, Univ. of London, London, 1985.

[14]Shyy, W., Tong, S. S., and Correa, S. M., "Numerical Recirculating Flow Calculations Using a Body-Fitted Coordinate System," *Numerical Heat Transfer*, Vol. 8, 1985, pp. 99–113.

[15]Rhie, C. M., and Chow, W. L., "Numerical Study of the Turbulent Flow Past and Airfoil with Trailing Edge Separation," *AIAA Journal*, Vol. 21, 1983, pp. 1525–1532.

[16]Chai, J. C., Lee, H. S., and Patankar, S. V., "Improved Treatment of Scattering Using the Discrete Ordinates Method," *Journal of Heat Transfer*, Vol. 116, No. 1, 1994, pp. 260–263.

[17]Chai, J. C., Parthasarathy, S., Lee, H. S., and Patankar, S. V., "A Finite-Volume Radiation Heat Transfer Procedure for Irregular Geometries," AIAA Paper 94-2095, June 1994.

[18]Siegel, R., and Howell, J. R., *Thermal Radiation Heat Transfer*, 3rd ed., McGraw-Hill, New York, 1993.

[19]Brigg, L. L., Miller, W. F., and Lewis, E. E., "Ray-Effect Mitigation in Discrete Ordinate-Like Angular Finite Element Approximations in Neutron Transport," *Nuclear Science and Engineering*, Vol. 57, 1975, pp. 205–217.

[20]Chai, J. C., Lee, H. S., and Patankar, S. V., "Evaluation of Spatial Differencing Practices for the Discrete-Ordinates Method," *Journal of Thermophysics and Heat Transfer*, Vol. 8, No. 1, 1994, pp. 140–144.

[21]Fiveland, W. A., "Discrete-Ordinates Solutions of the Radiative Transport Equation for Rectangular Enclosures," *Journal of Heat Transfer*, Vol. 106, No. 4, 1984, pp. 699–706.

[22]Truelove, J. S., "Discrete-Ordinates Solutions of the Radiation Transport Equation," *Journal of Heat Transfer*, Vol. 109, No. 1, 1988, pp. 1048–1051.

[23]Crosbie, A. L., and Schrenker, R. G., "Radiative Transfer in a Two-Dimensional Rectangular Medium Exposed to Diffuse Radiation," *Journal of Quantitative Spectroscopy and Radiative Transfer*, Vol. 31, No. 2, 1984, pp. 339–372.

[24]Menguc, M., and Viskanta, R., "Radiative Transfer in Three-Dimensional Rectangular Enclosures," *Journal of Quantum Spectroscopy and Radiative Transfer*, Vol. 33, No. 6, 1985, pp. 533–549.

[25]Fiveland, W. A., "Three-Dimensional Radiative Heat-Transfer Solutions by the Discrete-Ordinates Method," *Journal of Thermophysics and Heat Transfer*, Vol. 2, No. 4, 1988, pp. 309–316.

[26]Chai, J. C., "A Finite-Volume Method for Radiation Heat Transfer," Ph.D. Dissertation, Univ. of Minnesota, Minneapolis, MN, 1994.

[27]Kim, T.-K., and Lee, H. S., "Radiative Transfer in Two-Dimensional Anisotropic Scattering Media with Collimated Incidence," *Journal of Quantum Spectroscopy and Radiative Transfer*, Vol. 42, No. 3, 1989, pp. 225–238.

[28]Kim, T.-K., and Lee, H. S., "Effect of Anisotropic Scattering on Radiative Heat Transfer in Two-Dimensional Rectangular Enclosures," *International Heat and Mass Transfer*, Vol. 31, No. 8, 1988, pp. 1711–1721.

[29]Chai, J. C., Lee, H. S., and Patankar, S. V., "Treatment of Irregular Geometries Using a Cartesian-Coordinates-Based Discrete-Ordinates Method," *Radiative Heat Transfer—Theory and Applications*, HTD-Vol. 244, 1993, pp. 49–54.

[30]Sanchez, A., and Smith, T. F., "Surface Radiation Exchange for Two-Dimensional Rectangular Enclosures Using the Discrete-Ordinates Method," *Journal of Heat Transfer*, Vol. 114, No. 2, 1992, pp. 465–472.

[31]Chai, J. C., Lee, H. S., and Patankar, S. V., "Ray Effect and False Scattering in the Discrete Ordinates Method," *Numerical Heat Transfer*, Vol. 24, No. 4, Pt. B, 1993, pp. 373–389.